Redox modifier genes in amyotrophic lateral sclerosis in mice

Jennifer J. Marden,[1] Maged M. Harraz,[1] Aislinn J. Williams,[2] Kathryn Nelson,[1] Meihui Luo,[1] Henry Paulson,[2] and John F. Engelhardt[1]

[1]Department of Anatomy and Cell Biology, [2]Department of Neurology, and Graduate Program in Neuroscience, Carver College of Medicine, University of Iowa, Iowa City, Iowa, USA.

Amyotrophic lateral sclerosis (ALS), one of the most common adult-onset neurodegenerative diseases, has no known cure. Enhanced redox stress and inflammation have been associated with the pathoprogression of ALS through a poorly defined mechanism. Here we determined that dysregulated redox stress in ALS mice caused by NADPH oxidases Nox1 and Nox2 significantly influenced the progression of motor neuron disease caused by mutant SOD1^{G93A} expression. Deletion of either *Nox* gene significantly slowed disease progression and improved survival. However, 50% survival rates were enhanced significantly more by *Nox2* deletion than by *Nox1* deletion. Interestingly, female ALS mice containing only 1 active X-linked *Nox1* or *Nox2* gene also had significantly delayed disease onset, but showed normal disease progression rates. Nox activity in spinal cords from *Nox2* heterozygous female ALS mice was approximately 50% that of WT female ALS mice, suggesting that random X-inactivation was not influenced by *Nox2* gene deletion. Hence, chimerism with respect to Nox-expressing cells in the spinal cord significantly delayed onset of motor neuron disease in ALS. These studies define what we believe to be new modifier gene targets for treatment of ALS.

Introduction

Amyotrophic lateral sclerosis (ALS) is a fatal neurodegenerative disease that can be caused by dominant mutations in superoxide dismutase-1 (SOD1) (1). Great uncertainty remains as to the precise mechanism of motor neuron death in ALS, although oxidative stress and inflammation are both believed to be involved (2, 3). Transgenic mice overexpressing a mutant form of SOD1 found in ALS patients (SOD1^{G93A}) develop motor neuron disease similar to that seen clinically in familial forms of ALS. Recent studies using conditional reduction of mutant SOD1 in either motor neurons or glia of mice have suggested that both cell types influence different phases in the progression of motor neuron disease (4). Using bone marrow transplants or chimeric animals, other studies have demonstrated that mutant SOD1 expression in microglia leads to neuronal toxicity (5) and that non-neuronal cells lacking the mutant SOD1 protein can protect from disease (6). These findings strongly suggest that microglia significantly influence non–cell-autonomous damage of motor neurons.

Redox stress is thought to be an important component of disease progression in ALS (3, 7). Indeed, recent studies have shown that *SOD1^{G93A}* ALS transgenic mice produce elevated levels of Nox2^{gp91phox} and superoxide in spinal cord microglia (8). NADPH oxidases generate superoxide by transferring an electron from NADPH to molecular oxygen (9). Seven known NADPH oxidases (Nox1, Nox2, Nox3, Nox4, Nox5, Duox1, and Duox2) are thought to play important roles in redox-dependent cell signaling and/or inflammation (9). Although Nox2 expression increases in microglia of the spinal cord of *SOD1^{G93A}* transgenic mice, deletion of *Nox2* on a C57BL/6J inbred background of *SOD1^{G93A}* transgenic mice led to only a marginal increase in survival (122 to 135 days) (8). Hence, the possibility remains that other *Nox* genes may more significantly influence redox stress in ALS disease.

Nox1 and Nox2 are closely related homologs in the *Nox* gene family and share many of the same regulatory characteristics including a requirement for Rac1 and p22^{phox} coactivators (10–12). To this end, we performed studies comparing the contribution of *Nox2* or *Nox1* deletion on disease progression in mixed hybrid *SOD1^{G93A}* ALS mice. Because both *Nox* genes reside on the X chromosome, we evaluated all *Nox* genotypes for male (WT, *Nox$^{X+/Y}$*; and KO, *Nox$^{X-/Y}$*) and female (WT, *Nox$^{X+/X+}$*; heterozygous [HET], *Nox$^{X+/X-}$*; and KO, *Nox$^{X-/X-}$*) mice on the *SOD1^{G93A}* transgenic background, using siblings from F2 generations. The onset and progression of motor neuron disease were monitored using rotarod performance, stride length, weight, motor neuron counts, and/or survival as indices. Here we show that disrupting either of these NADPH oxidase genes (*Nox1* or *Nox2*) significantly delayed the progression of motor neuron disease in a *SOD1^{G93A}* transgenic mouse model of ALS. Interestingly, female ALS mice lacking a single copy of the X-chromosomal *Nox1* or *Nox2* genes also exhibited significantly increased survival rates. Thus, we conclude that in the setting of random X-inactivation, a 50% reduction in *Nox1*- or *Nox2*-expressing cells has a substantial therapeutic benefit in ALS mice. These studies demonstrate that multiple *Nox* genes appear to contribute to the pathoprogression of ALS and expand potential therapeutic targets for this disease.

Results and Discussion

Gene deletion of Nox1 or Nox2 increases survival and slows disease progression in SOD1^{G93A} transgenic mice. Given that enhanced redox stress has been associated with disease progression in ALS mouse models, we sought to evaluate 2 potential *Nox* genes responsible for ROS generation in hemizygous *SOD1^{G93A}* transgenic mice and their affect on the progression of motor neuron disease. We bred female *Nox1*-KO and *Nox2*-KO mice to hemizygous male *SOD1^{G93A}* ALS mice

Nonstandard abbreviations used: ALS, amyotrophic lateral sclerosis; CT, threshold cycle; HET, heterozygous; SOD, superoxide dismutase.

Conflict of interest: The authors have declared that no conflict of interest exists.

Citation for this article: *J. Clin. Invest.* **117**:2913–2919 (2007). doi:10.1172/JCI31265.

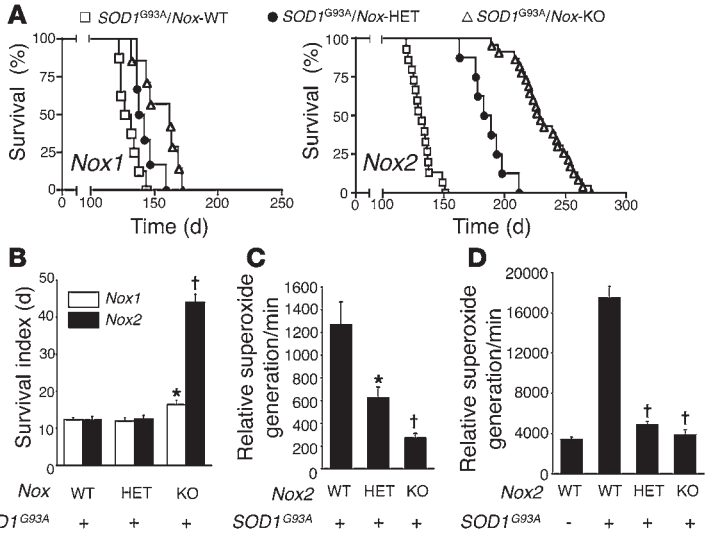

Figure 1

Deletion of NADPH oxidase genes (*Nox1* or *Nox2*) enhances survival and survival index in ALS mice and significantly reduces superoxide production in spinal cords of end-stage *SOD1*^{G93A} mice. (**A**) Survival curves for hemizygous *SOD1*^{G93A} transgenic mice with the indicated *Nox1* and *Nox2* genotypes. Median 50% survival rates were as follows: *Nox1*-WT (n = 8), 129 days; *Nox1*-HET (n = 6), 140 days, $P < 0.03$ versus *Nox1*-WT; *Nox1*-KO (n = 7), 162 days, $P < 0.004$ versus *Nox1*-WT; *Nox2*-WT (n = 16), 132 days; *Nox2*-HET (n = 8), 186 days, $P < 0.0001$ versus *Nox2*-WT; *Nox2*-KO (n = 24), 229 days, $P < 0.0001$ versus *Nox2*-WT. (**B**) Survival index for mice in **A**; onset of disease was defined as 10% weight loss from peak weight. Values are mean ± SEM. *P = 0.059, †$P < 0.0001$ versus WT. (**C** and **D**) NADPH-dependent superoxide production in spinal cords of hemizygous *SOD1*^{G93A} transgenic mice with WT, HET, and KO *Nox2* genotypes. The relative mean rate ± SEM of superoxide production is plotted. (**C**) Ages at the time of spinal cord harvest were as follows: *Nox2*-WT, 125, 132, and 124 days; *Nox2*-HET, 186, 179, and 183 days; *Nox2*-KO, 224, 223, and 242 days (n = 3 per genotype). All mice were at the stage of clinical death at the time of harvest. †$P < 0.008$, *$P < 0.045$ versus WT; Student's t test. (**D**) All mice were harvested at 120 days of age (n = 4 per genotype). †$P < 0.0001$ versus WT; Student's t test.

(Supplemental Figures 1 and 2; supplemental material available online with this article; doi:10.1172/JCI31265DS1) and evaluated siblings from the F2 generation for the development of motor neuron disease. F2 generations were necessary to capture all possible genotypes in both male and female siblings, because both *Nox1* and *Nox2* are on the X chromosome. Mutant *SOD1* transgene copy number was also stable throughout the F2 generations, as determined by real-time quantitative PCR (Supplemental Figure 3). The *Nox1* and *Nox2* mice were both maintained on the C57BL/6 background; however, only the *Nox2* mice were inbred to greater than 13 generations (*Nox1* KO mice were backcrossed about 7 generations onto the C57BL/6 background). Unlike a previous study evaluating deletion of the *Nox2* gene in *SOD1*^{G93A} C57BL/6J inbred transgenic mice (8), our study used *SOD1*^{G93A} B6SJL mice on a mixed hybrid background (F1 hybrids from a C57BL/6J × SJL cross).

Homozygous deletion of either *Nox1* or *Nox2* significantly delayed the death of hemizygous *SOD1*^{G93A} ALS mice (Figure 1A). *Nox2* gene deletion had the greatest impact on survival in both male and female mice (*Nox2*-WT, 132 days; *Nox2*-KO, 229 days) and also led to a 4-fold increase in the survival index (time to death after disease onset; Figure 1B). The finding of an increased survival index in *Nox2*-KO *SOD1*^{G93A} transgenic mice is significant because, to our knowledge, no other single modifier genes have previously been found that affect survival index. Nox1-deficient mice gave rise to a much smaller, but still significant, protective effect in terms of survival (*Nox1*-WT, 129 days; *Nox1*-KO, 162 days), but not survival index (Figure 1, A and B).

Given the significant 97-day increase in survival of *Nox2*-KO *SOD1*^{G93A} B6SJL mice in our study compared with the 13-day increase observed in a previous study using *Nox2*-KO *SOD1*^{G93A} congenic C57BL/6J mice (8), we investigated the Nox2 dependence of several disease-associated phenotypes at the cellular level. Enhanced survival of ALS *Nox2*-KO mice correlated with higher motor neuron counts in the lumbar region of the spinal cord at 120 days and reduced expression of the activated microglial marker CD11b (Figure 2). Deletion of *Nox2* also resulted in reduced redox stress in spinal cords of 120-day-old mice, as evidenced by reduced dihydroethidium staining for superoxide and protein carbonylation (Supplemental Figure 4). These findings were similar to those observed in the previous *Nox2*-KO *SOD1*^{G93A} congenic C57BL/6J study (8). Furthermore, NADPH-dependent superoxide production from spinal cord total endomembranes at 120 days (Figure 1C) and clinical death (Figure 1D) were both significantly reduced in *Nox2*-KO *SOD1*^{G93A} mice compared with *Nox2*-WT *SOD1*^{G93A} mice.

Examination of rotarod performance and stride length substantiated the finding of decreased motor neuron disease in male and female *Nox2*-KO ALS mice (Figure 3, B–D). A decline in rotarod performance and stride length was accompanied by hind-limb muscle atrophy, a hallmark of disease progression in ALS mice. To determine whether Nox2 deficiency protected *SOD1*^{G93A} mice from muscle atrophy, the weight, fiber area, and fiber number of the peroneus longus muscles was evaluated. At 100 days, *Nox2*-KO *SOD1*^{G93A} mice demonstrated significant protection from loss in hind-limb muscle mass compared with *Nox2*-WT *SOD1*^{G93A} mice (Supplemental Figure 5, A and B). These differences in muscle mass between the *Nox2* genotypes of *SOD1*^{G93A} mice correlated with changes in muscle fiber area (Supplemental Figure 5, C and D). Furthermore, *Nox2*-KO *SOD1*^{G93A} mice were indistinguishable from nontransgenic littermates for both these muscle parameters (Supplemental Figure 5).

Breeding of hemizygous *SOD1*^{G93A} B6SJL mice onto the C57BL/6 background has previously been shown to increase survival by approximately 13 to 14 days (*SOD1*^{G93A} B6SJL hybrid mice, 130.2 ± 11.2 days; *SOD1*^{G93A} C57BL/6 congenic mice, 143.6 ± 7.5 days; ref. 13). A second study performing the same analysis demonstrated increases in survival averaging 28 days when comparing *SOD1*^{G93A} B6SJL hybrid mice (128.9 ± 9.1 days) with *SOD1*^{G93A} C57BL/6J congenic mice (157.1 ± 9.3 days) (14). Both of these studies demonstrate that C57BL/6 modifier genes can slow disease progression in ALS mice. However, the mean survival times for *Nox*-WT *SOD1*^{G93A} mice seen in our studies (129 and 132 days for *Nox1* and *Nox2* backgrounds, respectively) were very similar to *SOD1*^{G93A} B6SJL hybrid mice in these previous reports. Because a previous study using inbred C57BL/6 *Nox2*-KO *SOD1*^{G93A} mice demonstrated much smaller increases in survival (8) compared with our mixed B6SJL background *Nox2*-KO *SOD1*^{G93A} mice, we hypothesize that multiple SJL-derived modifier genes likely act in concert with Nox2 deficiency

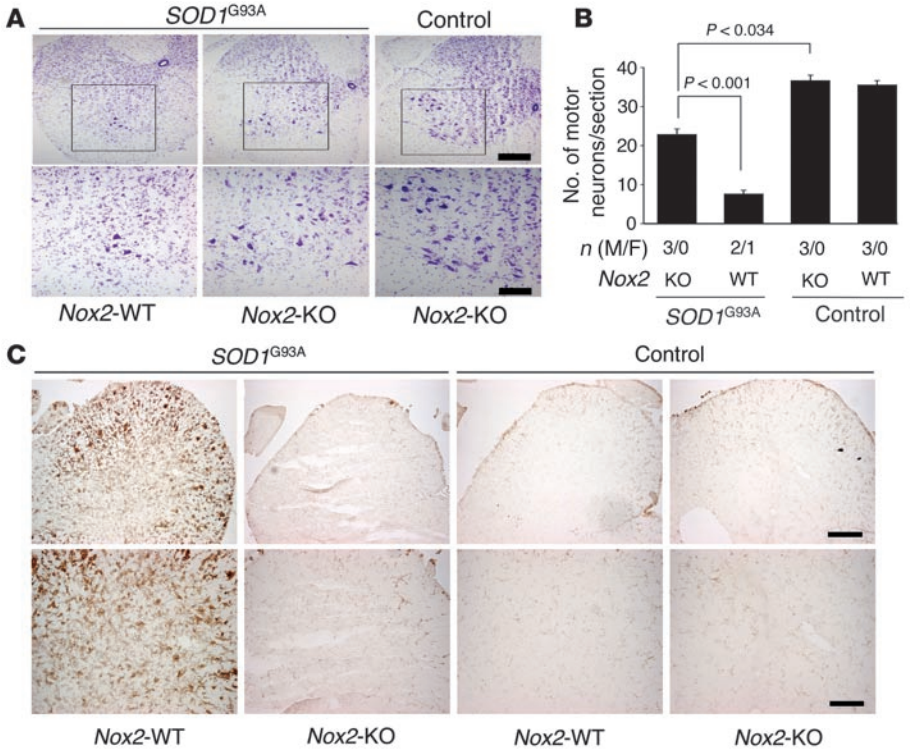

Figure 2
Nox2 deficiency rescues motor neuron death in the spinal cords of mice hemizygous for the *SOD1*^{G93A} transgene. Motor neurons were quantified in the lumbar region of the spinal cord using Cresyl violet staining at 120 days for the following genotypes: *SOD1*^{G93A}/*Nox2*-WT, *SOD1*^{G93A}/*Nox2*-KO, *Nox2*-WT, and *Nox2*-KO. In total 3 animals were included in each group and they were all derived from the same breeder pair (2 independent litters). (**A**) Representative photomicrographs of spinal cord section stained in Cresyl violet. Bottom panels show higher-magnification views of the boxed regions above. (**B**) Morphometric data on motor neuron counts for the given genotypes. Results depict the mean ± SEM for the indicated number of male and female animals quantified in each group. (**C**) Immunohistochemical staining for CD11b in spinal cords of the same mice shown in **A**. Scale bars: 200 μm (**A** and **C**, upper panels); 100 μm (**A** and **C**, lower panels).

to significantly enhance survival of *SOD1*^{G93A} mice. In support for this hypothesis, we did not observe a high degree of variability in survival among siblings for the various *Nox1* and *Nox2 SOD1*^{G93A} genotypes in the F1 and F2 generations (Supplemental Figures 1 and 2), suggesting that a single modifier gene could not account for increased survival associated with the *Nox* mutant alleles. An embryonic stem cell–derived 129 segment linked to the *Nox2* gene deletion near the telomere of the X chromosome likely segregates with the *Nox2* mutant allele. However, a single modifier gene in this region is also unlikely to account for the increased survival seen in the B6SJL *Nox2*-KO *SOD1*^{G93A} mice for 2 reasons. First, studies that have evaluated 129 modifier genes on the *SOD1*^{G86R} C57BL/6 background suggest that they do not exist on the X chromosome, but rather on chromosome 13 between D13mit36 and D13mit76 (15). Second, this 129-derived segment linked to the targeted *Nox2* allele on the telomere of the X chromosome would certainly also be present in the previous study that used inbred C57BL/6 *Nox2*-KO *SOD1*^{G93A} mice (8). Because we used the same inbred C57BL/6 *Nox2*-KO mice for breeding, yet observed widely divergent survival rates of *Nox2*-KO *SOD1*^{G93A} mice, it is unlikely this 129-linked segment can solely account for differences in survival between these 2 studies.

Female SOD1^{G93A} *transgenic mice heterozygous for X-linked Nox genes have increased survival but unaltered survival index.* Interestingly, *Nox2*-HET female ALS mice also demonstrated significant increases in survival (*Nox2*-WT, 132 days; *Nox2*-HET, 186 days; Figure 1A and Figure 3A), although they lacked a corresponding increase in survival index (Figure 1B). There was also a limited but significant heterozygous effect on increased survival in *Nox1*-HET female ALS mice (Figure 1A). Furthermore, the results of our rotarod performance and stride-length analyses substantiated the finding of decreased motor neuron disease in female *Nox2*-HET ALS mice (Figure 3, B–D). Both *Nox1* and *Nox2* genes reside on the X chromosome. In female somatic cells, a single X chromosome is inactivated to maintain the correct dosage of genes expressed from the X chromosome (16). Hence, in the absence of a selective bias, female mice heterozygous for these *Nox* genes would be expected to have 50% normal cells (with one active *Nox* gene) and 50% defective cells (with no active *Nox* gene). However, biased X chromosome inactivation has been previously reported in female patients with X-linked chronic granulomatous disease caused by *Nox2* gene mutations (17). Given the significant protective effect seen in *Nox2*-HET female mice, we sought to determine how dosage of Nox2 activity in the spinal cord might influence disease progression in ALS mice. In mice with end-stage disease, Nox activity in the spinal cords of female *Nox2*-HET *SOD1*^{G93A} mice fell between that of female *Nox2*-KO and *Nox2*-WT *SOD1*^{G93A} mice (Figure 1C). This suggests that X-inactivation likely occurs randomly in female *Nox2*-HET *SOD1*^{G93A} mice, with about 50% of the microglia and neuronal cell types predicted to be deficient for Nox2 function. These findings demonstrate that a 50% reduction of Nox2 activity in the spinal cord has a significant impact on survival of ALS mice.

It is presently unclear why chimerism for Nox2 expression in the spinal cord significantly influences survival, but not the survival index, in female *SOD1*^{G93A} transgenic mice. Interestingly, other reports generating chimeric mice composed of mixtures of normal and SOD1 mutant–expressing non-neuronal cells significantly attenuated toxicity associated with mutant-expressing motor neurons (6). Given that Nox2 is highly expressed in microglia of *SOD1*^{G93A} transgenic mice (8), chimerism of *Nox2* gene expression in microglia appears to influence disease progression. It has been postulated that the ALS phenotype is at least partially dictated by an altered redox-balance within cells expressing the mutant SOD1 through an as-yet undefined gain of function (2, 3). A recent study

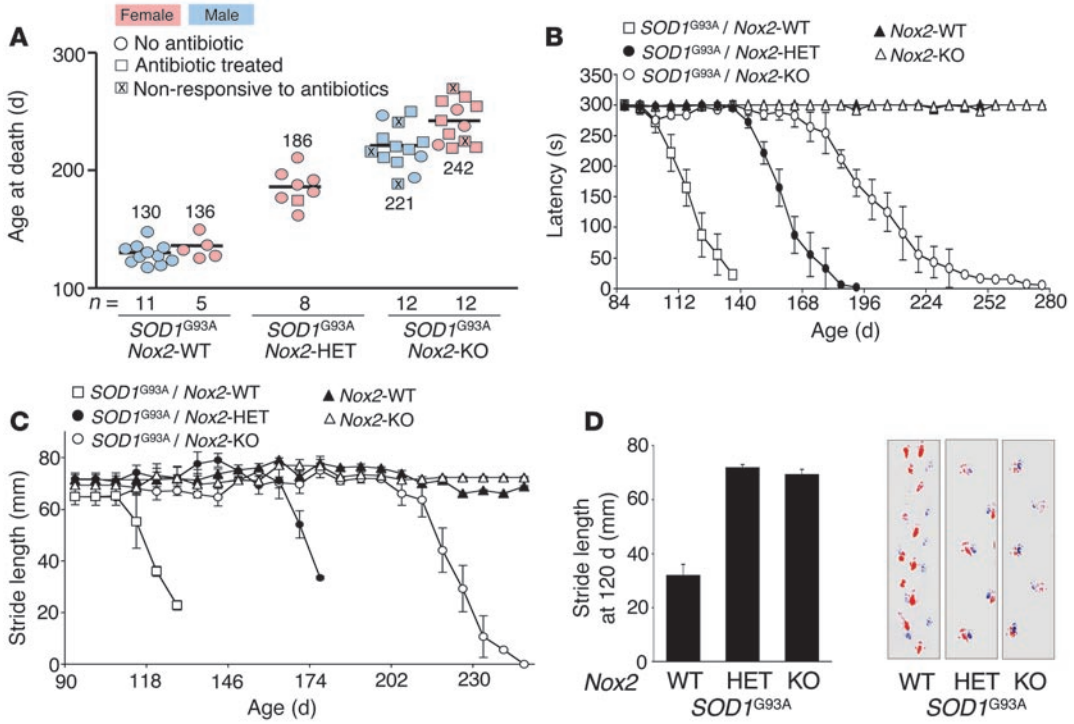

Figure 3
Disease phenotyping of *Nox2* genotypes on the *SOD1^{G93A}* ALS background. (**A**) Survival data of male and female mice for the given genotypes. Boxes denote mice treated for eye infections with antibiotics; those marked with an X denote mice that were unsuccessfully treated and died from eye infections. Circles denote mice that never contracted eye infection. Numbers denote mean survival in days. (**B**) Rotarod data demonstrating the mean latency time maintained on the rotarod for each given genotype as a function of age. Results are mean ± SEM for the same mice as in **A**. (**C**) Stride length data demonstrating the mean stride distance for each given genotype as a function of age. Results are mean ± SEM for the same mice as in **A**. (**D**) Mean stride lengths at 120 days for the indicated genotypes. Representative raw stride length data is shown at right.

using conditional elimination of mutant SOD1 in neurons or glial cells has also demonstrated that these cell types control early and later phases of disease, respectively (4). In the context of these other findings, our current data demonstrating significantly enhanced survival in female ALS mice with chimeric Nox2 expression suggest that SOD1^{G93A} expression in microglia may directly influence deleterious cell-autonomous function of Nox2.

Nox2 deficiency leads to an enhanced predisposition to lethal eye infections in SOD1^{G93A} transgenic mice. Notably, in the *Nox2*-KO *SOD1^{G93A}* transgenic background, we observed a high frequency of eye disease that rapidly led to death within 1 week, without the typical progression of motor defects. Cultures of eye secretions from affected mice were positive for *Staphylococcus aureus*. These infections were never observed in *Nox2*-KO littermates lacking the *SOD1^{G93A}* transgene. Systemic treatment with antibiotics reversed this eye disease in about 75% of affected mice (Figure 3A). Importantly, antibiotic treatment of control ALS mice on the WT *Nox2* background did not alter either the progression of motor neuron deficits or survival (data not shown). The etiology of these eye infections remains unclear, and histopathologic analysis oddly revealed little signs of inflammation (Supplemental Figure 6). Of note, there was rapid accumulation of secretions around the eye from affected *Nox2*-KO *SOD1^{G93A}* transgenic mice suffering from infections (Supplemental Figure 6A).

Histopathology revealed 2 consistent abnormalities in 2 ocular glands (the Harderian gland and lacrimal gland) of affected *Nox2*-KO *SOD1^{G93A}* transgenic mice compared with *Nox2*-WT *SOD1^{G93A}* transgenic mice (n = 3 per group). First, the Harderian gland of *Nox2*-WT *SOD1^{G93A}* transgenic mice always contained accumulated porphyrin aggregates in the lumen of glandular tubules that were never seen in affected *Nox2*-KO *SOD1^{G93A}* transgenic mice (Supplemental Figure 6, C and F). The function of the Harderian gland, which is unique to rodents (18), remains unclear. However, this structure has been proposed to be a source of lubricant and to be involved in immune responses of the eye (19). Hence it is possible that altered secretions from the Harderian gland of affected *Nox2*-KO *SOD1^{G93A}* transgenic mice influence the observed increased predisposition to bacterial eye infections. Second, abnormalities in the cellular architecture of the lacrimal glands were also observed in affected *Nox2*-KO *SOD1^{G93A}* transgenic mice (Supplemental Figure 6, D and G). The lacrimal glands have also been proposed to play a role in innate immunity of the eye surface and express several antibacterial proteins (20). Hence, defective function of both the Harderian gland and the lacrimal glands may account for increased incidence of infection in eyes of *Nox2*-KO *SOD1^{G93A}* transgenic mice.

It is presently unclear why overexpression of SOD1^{G93A} manifests these abnormalities only on the *Nox2*-KO background. However, the findings imply potential new functions for both SOD1 and Nox2 in eye innate immunity. Given the rapid nature of death when infected mice were not treated with antibiotics, we hypothesize that retroorbital infection of the brain were rapidly occurring and leading to death. Compromised immune function in

Nox2-KO animals likely contributed to the lack of inflammation in these infections. While it might be tempting to dismiss these eye infections as being the result of opportunistic infection due to poor hygiene of the animal caused by hind-limb impairment, it is important to note that infections occurred on average 17.7 ± 6.5 days prior to the onset of disease symptoms as determined by a 10% loss of peak body weight (Supplemental Figure 7A). There was also limited hind-limb impairment at the time of infection (Supplemental Figure 7B). Hence, impaired grooming cannot explain why the infection was only present in the ALS *Nox2*-KO mice.

Conclusions. Microglia are considered to be regulators of the immune system in the central nervous system. Under normal conditions, microglia respond to areas of damage. However, overactivation of microglia can lead to the production of proinflammatory cytokines and ROS, which have been associated with neuroinflammation that can further perpetuate neurodegeneration. Among the factors produced by activated microglia, ROS could potentially enhance neurodegeneration by at least 2 mechanisms. First, ROS can cause direct damage to neurons. Second, increases in the intracellular concentrations of ROS may activate proinflammatory signaling cascades that result in the activation of more microglia. Other laboratories have shown that there is an upregulation of microglia during the progression of ALS disease, and that in *Nox2*-KO mice there is a marked decrease in the number of activated microglia following LPS treatment (21). This suggests that ROS generated from NADPH oxidases play a role in signaling events leading to microglia activation. The goal of this study was to determine the effect of NADPH oxidase–derived superoxide in ALS disease progression in transgenic mice. We demonstrated increased survival and delayed disease onset when 2 related *Nox* genes, *Nox1* and *Nox2*, were deleted. These findings substantiate a growing body of literature implicating *Nox* genes in proinflammatory processes associated with inherited and acquired diseases. Interestingly, our findings in female $SOD1^{G93A}$ transgenic mice heterozygous for the *Nox2* X-linked gene, and hence containing 50% Nox2-inactive cells, suggest that the interplay between Nox-activated microglia and neuronal cell types in ALS may be more complex than previously thought.

It is currently unclear why an earlier study (8) failed to find substantial protection against motor neuron defects in *Nox2*-KO $SOD1^{G93A}$ transgenic mice. This is especially perplexing given that the physiological and redox stress data were extremely similar between the previous study and the present one. However, untreated eye infections leading to premature death and/or differences in the genetic background of the mice studied could potentially account for these discrepancies. Indeed, genetic background has previously been shown to influence survival of ALS mice (13), and this could have accounted for the observed differences. However, the marginal increase in life span seen in the *Nox1*-KO compared with the *Nox2*-KO ALS mice would suggest that modifier genes must act in concert with Nox2 deficiency to provide substantial improvements in survival. The potential existence of additional modifier genes that may influence Nox2 function in ALS would be particularly relevant to human ALS disease, which manifests considerable phenotypic variability.

The findings presented here have important implications for several reasons. First, we believe the demonstrated increase in survival of ALS mice is the largest ever reported as a consequence of disrupting a single gene (*Nox2*). Second, these studies also demonstrate that more than 1 *Nox* gene (*Nox1* and *Nox2*) can influence disease progression in ALS mice. Third, to our knowledge, no other single modifier gene deletions have been shown to significantly delay disease progression in ALS mice (i.e., survival index). Finally, our findings in female ALS mice suggest that a 50% reduction in Nox2 activity can significantly alter the progression of disease in this $SOD1^{G93A}$ transgenic model of ALS. Our findings suggest that targeted inhibition of Nox pathways using pharmacologic-based approaches could provide significant benefits for ALS patients.

Methods

Animal models and breeding schemes. Three mouse strains were used in these studies. (a) Transgenic mice overexpressing the human $SOD1^{G93A}$ mutant (22) were used as a model of ALS [strain name, B6SJL-Tg($SOD1^{G93A}$)1Gur/J; stock no. 002726; The Jackson Laboratory]. The strain was maintained by breeding hemizygous carrier males to B6SJLF1 hybrid females (i.e., mixed C57BL/6 and SJL background). Only hemizygous carrier male and females were used in phenotyping studies and had life spans of 19–23 weeks. (b) $Nox2^{gp91phox}$ KO mice (23) were also obtained from The Jackson Laboratory (strain name, B6.129S6-$Cybb^{tm1Din}$/J; stock no. 002365) and were inbred on the C57BL/6 background. (c) *Nox1* KO mice (24) were a kind gift from K.H. Krause (University of Geneva, Geneva, Switzerland) and B. Banfi (University of Iowa). This line has an undefined background consisting of a mixed C57BL/6 and 129SvJ lineage. The generation of $SOD1^{G93A}$ transgenic mice on the *Nox2*-KO or *Nox1*-KO backgrounds were achieved using the following breeding scheme. Because both *Nox2* and *Nox1* genes are on the X chromosome, 2 rounds of breeding were required to obtain all possible genotypes in each sex (*Nox*-HET males were the only genotype not attainable). Hemizygous $SOD1^{G93A}$ transgenic males were bred to $Nox2^{-/-}$ or $Nox1^{-/-}$ females. *Nox*-HET females were used for the next round of breeding against $SOD1^{G93A}$ hemizygous *Nox*-KO males (i.e., $Nox2^{+/-} \times SOD1^{G93A}/Nox2^{-/Y}$ or $Nox1^{+/-} \times SOD1^{G93A}/Nox1^{-/Y}$) to give rise to mixed litters containing *Nox*-KO (male and female), *Nox*-HET (female only), and *Nox*-WT (male only) genotypes, either lacking or hemizygous for the $SOD1^{G93A}$ transgene. Similarly, *Nox*-HET females were also bred against $SOD1^{G93A}$ hemizygous *Nox*-WT males (i.e., $Nox2^{+/-} \times SOD1^{G93A}/Nox2^{+/Y}$ or $Nox1^{+/-} \times SOD1^{G93A}/Nox1^{+/Y}$) to give rise to mixed litters containing *Nox*-KO (male only), *Nox*-HET (female only), and *Nox*-WT (male and female) genotypes either lacking or hemizygous for the $SOD1^{G93A}$ transgene. Genotyping for *Nox2* and $SOD1^{G93A}$ mice was performed by standard PCR protocols using primer sets designed by The Jackson Laboratory. *Nox1* PCR genotypes were performed as previously described (24). Animal procedures were performed in accordance with NIH guidelines and were approved by the University of Iowa Institutional Animal Care and Use Committee.

Real-time quantitative PCR determination of $SOD1^{G93A}$ transgene copy number. Changes in transgene copy number were evaluated using real-time quantitative PCR by determining the difference in threshold cycle (ΔCT) between the transgene (*hSOD1*) and a reference gene (*mIL2*) following a previously published protocol (25). The following primers were used for the transgene *hSOD1*: forward, 5′-CATCAGCCCTAATCCATCTGA-3′; reverse, 5′-CGCGACTAACAATCAAAGTGA-3′. The following primers were used for the reference gene *mIL2*: forward, 5′-CTAGGCCACAGAATTGAAAGATCT-3′; reverse, 5′-GTAGGTGGAAATTCTAGCATCATCC-3′. The final concentration of the primers for *hSOD1* and *mIL2* were 0.4 and 0.5 μM, respectively. The Brilliant SYBR Green QPCR Master Mix reagent (Stratagene) was used for real-time amplification. EcoRI-digested genomic DNA (10 ng) was used in each reaction. After a 10-minute initial cycle at 95°C, 40 PCR cycles of 95°C for 30 seconds, 60°C for 1 minute, and 72°C for 30 seconds were performed. Assays were run in duplicate using an iCycler (Bio-Rad). The ΔCT was calculated as

the difference between the human *SOD1* CT and the mouse *IL2* CT for all mice in the *Nox2* F2 generation. The ΔCT value was used to calculate transgene copy number for each mouse in the cohort using the reported copy number (24) and ΔCT (6.967) of the B6SJL-TgN(*SOD1*^{G93A})1Gur as known values (26). The unknown copy number was computed as the copy number of the known type times $2^{\Delta\delta CT}$, where ΔδCT equals the ΔCT of the unknown minus the ΔCT of the known.

Disease phenotyping. B6SJL-Tg(*SOD1*^{G93A})1Gur/J mice hemizygous for a highly expressed mutant *SOD1*^{G93A} transgene develop disease onset at approximately 110 days of age and usually die within 2 weeks. In our hands, 50% survival was 123 days for B6SJL-Tg(*SOD1*^{G93A})1Gur/J males (n = 30) and 128 days for females (n = 33). Because phenotyping involved rotarod performance, which was indirectly affected by extremes in body weight, an inclusion criterion of 20–40 g body weight prior to the onset of disease was used for inclusion of mice in survival and phenotyping studies. Four mice fell out of the study because their presymptomatic weight exceeded 40 g: 2 *Nox2*-WT, 1 *Nox2*-HET, and 1 *Nox2*-KO. None of the mice on the *Nox1*-KO background failed the weight criteria. Clinical death was defined as the time when the mice could no longer right themselves within 20 seconds of being placed on their backs or when they lost 20% of their body weight within a 1-week period. If either of these criteria were met, the mice were euthanized. At the onset of hind-limb paralysis, mice were grueled, and during the terminal stage of disease, they were individually housed. *Nox2*-KO mice also hemizygous for the *SOD1*^{G93A} transgene were susceptible to superficial eye infections. At the first sign of discharge, mice were placed on water or gruel containing antibiotics (0.1 mg/ml gentamicin and 0.1 mg/ml ceftazidime). If the condition worsened, mice were additionally injected subcutaneously with 85 mg/kg of enterfloxin (Baytril) once per day for 14 days. To insure that antibiotic treatment did not alter the course of disease, *SOD1*^{G93A}/*Nox2*-WT mice were put on antibiotic water at 90 days and monitored for survival, which did not significantly change (untreated, 133 ± 4 days; treated, 131 ± 2 days; n = 6 per group). Eye infection in *Nox2*-HET females hemizygous for the *SOD1*^{G93A} transgene was only observed in 1 of the 8 females analyzed and was never observed in *Nox2*-KO mice lacking the *SOD1*^{G93A} transgene.

Nox activity assays in spinal cord endomembranes. Spinal cords were lysed in homogenization buffer (50 mM Tris-HCl, 320 mM sucrose, and 1 mM EDTA, pH 7.4) by nitrogen cavitation. Cell lysate (600 μg) was centrifuged at 3,000 *g* to remove the heavy mitochondria and nuclei to generate a postnuclear supernatant (PNS). The PNS was subsequently centrifuged at 100,000 *g* for 1 hour to spin down total membranes. The membranes were washed 3 times in homogenization buffer before being resuspended in 100 μl of homogenization buffer and used to measure NADPH-dependent superoxide production. NADPH oxidase activities were analyzed by measuring the rate of superoxide generation using a chemiluminescent, lucigenin-based system (27) with modification as previously described (28). Lucigenin (5 μM) in 50 μl of total membrane was incubated in the dark at room temperature for 15 minutes. Lucigenin chemiluminescence (LCL) was measured using a single-tube Luminometer TD20-20 (Turner Designs). The reaction was initiated by the addition β-NADPH to a final concentration of 100 μM. LCL was measured over the course of 5 minutes. The initial slope of the luminescence curve (RLU/min) was used to calculate the rate of luminescence product formation and compared between samples as an index of NADPH oxidase activity. In the absence of NADPH, the luminescence was negligible and did not change over time.

Physiologic assays for disease. Beginning at 80 days of age, mice were evaluated by 3 criteria for the onset of motor neuron defects and disease symptoms: (a) weight, (b) rotarod performance, and (c) stride length. Weight was measured weekly. Mice were analyzed by rotarod weekly (Ugo Bastile) using 3 trials performed during the light phase of the 12-hour light/12-hour dark cycle for each mouse. The average duration was recorded. Time was stopped when the mouse fell from the rod or after an arbitrary limit of 300 seconds. Footprint analysis was also performed every 7–14 days. Mouse front and hind paws were covered in different-colored paint to record walking patterns during continuous locomotion. Stride length was measured, and the mean stride length was calculated from at least 6 consecutive strides (29).

Cresyl violet staining of spinal cord and motor neuron counts. Mice were anesthetized deeply with a combination of 150 mg/g ketamine and 15 mg/g xylazine in sterile PBS and perfused transcardially with 20 ml filtered cold PBS followed by 20 ml 4% paraformaldehyde. Spinal cords were harvested, placed into 4% paraformaldehyde, and kept at 4°C overnight. Cords were then stored in sterile PBS at 4°C for at least 24 hours before cryoprotection in 30% sucrose overnight. The lumbar spinal cord was removed from the remainder of the spinal cord and cut into 4-mm-long segments. Segments were embedded in OTC freezing medium and sectioned axially at 20 μm at –35°C with a Microm Cryostat II equipped with the Cryo-Jane System (Instrumedics Inc.) for preservation of tissue structure. Every fifth section was stained with 0.1% (w/v) cresyl violet acetate (Nissl stain) without counterstain (30). Motor neurons in the ventral horn were quantified by counting large pyramidal neurons that stain with cresyl violet and possess a prominent nucleolus. At least 11 sections of spinal cord were counted per mouse, and the analysis was performed blindly. Three animals per genotype were analyzed.

Immunohistochemistry. Mouse spinal cords were fixed as described above for the cresyl violet–stained sections. Activated microglia were immunostained using a CD11b antibody from AbD Serotec Inc. at a 1:100 dilution. Peroxidase-labeled secondary antibody was detected using DAB.

Measurement of protein oxidation. Protein carbonyls were detected in spinal cord lysates made from the lumbar region of 120-day-old *SOD1*^{G93A} *Nox2*-WT, *SOD1*^{G93A} *Nox2*-KO, and nontransgenic mice. Immunoblot detection of carbonyl groups introduced into proteins by derivatization of spinal cord homogenates with 2,4 dinitrophenylhydrazine was performed using the Oxyblot protein oxidation kit as specified by the manufacturer (Chemicon Inc.)

Statistics. Statistical significance for all comparisons, with the exception of survival curves, was assessed using ANOVA followed by an unpaired, 2-tailed Student's t test. Kaplan-Meier survival curves were generated using Prism software and compared using the log-rank test; resulting P values are 2-tailed. A P value less than 0.05 was considered significant.

Acknowledgments

The authors thank Kem Singletary for help and advice in monitoring and treating the mice used in this study. This work was supported by NIH grants DK067928 and DK54759 from the Gene Therapy Core Center. J.F. Engelhardt is the Roy J. Carver Chair of Molecular Medicine.

Received for publication December 17, 2006, and accepted in revised form June 29, 2007.

Address correspondence to: John F. Engelhardt, Department of Anatomy and Cell Biology, Carver College of Medicine, University of Iowa, 51 Newton Road, Room 1-111 BSB, Iowa City, Iowa 52242, USA. Phone: (319) 335-7744; Fax: (319) 335-7198; E-mail: john-engelhardt@uiowa.edu.

Henry Paulson's present address is: Department of Neurology, University of Michigan Medical Center, Ann Arbor, Michigan, USA.

1. Rosen, D.R., et al. 1993. Mutations in Cu/Zn superoxide dismutase gene are associated with familial amyotrophic lateral sclerosis. *Nature.* **362**:59–62.
2. Bruijn, L.I., Miller, T.M., and Cleveland, D.W. 2004. Unraveling the mechanisms involved in motor neuron degeneration in ALS. *Annu. Rev. Neurosci.* **27**:723–749.
3. Pasinelli, P., and Brown, R.H. 2006. Molecular biology of amyotrophic lateral sclerosis: insights from genetics. *Nat. Rev. Neurosci.* **7**:710–723.
4. Boillee, S., et al. 2006. Onset and progression in inherited ALS determined by motor neurons and microglia. *Science.* **312**:1389–1392.
5. Beers, D.R., et al. 2006. Wild-type microglia extend survival in PU.1 knockout mice with familial amyotrophic lateral sclerosis. *Proc. Natl. Acad. Sci. U. S. A.* **103**:16021–16026.
6. Clement, A.M., et al. 2003. Wild-type nonneuronal cells extend survival of SOD1 mutant motor neurons in ALS mice. *Science.* **302**:113–117.
7. Barber, S.C., Mead, R.J., and Shaw, P.J. 2006. Oxidative stress in ALS: a mechanism of neurodegeneration and a therapeutic target. *Biochim. Biophys. Acta.* **1762**:1051–1067.
8. Wu, D.C., Re, D.B., Nagai, M., Ischiropoulos, H., and Przedborski, S. 2006. The inflammatory NADPH oxidase enzyme modulates motor neuron degeneration in amyotrophic lateral sclerosis mice. *Proc. Natl. Acad. Sci. U. S. A.* **103**:12132–12137.
9. Lambeth, J.D. 2004. NOX enzymes and the biology of reactive oxygen. *Nat. Rev. Immunol.* **4**:181–189.
10. Ueyama, T., Geiszt, M., and Leto, T.L. 2006. Involvement of Rac1 in activation of multicomponent Nox1- and Nox3-based NADPH oxidases. *Mol. Cell. Biol.* **26**:2160–2174.
11. Cheng, G., Diebold, B.A., Hughes, Y., and Lambeth, J.D. 2006. Nox1-dependent reactive oxygen generation is regulated by Rac1. *J. Biol. Chem.* **281**:17718–17726.
12. Park, H.S., et al. 2004. Sequential activation of phosphatidylinositol 3-kinase, beta Pix, Rac1, and Nox1 in growth factor-induced production of H2O2. *Mol. Cell. Biol.* **24**:4384–4394.
13. Heiman-Patterson, T.D., et al. 2005. Background and gender effects on survival in the TgN(SOD1-G93A)1Gur mouse model of ALS. *J. Neurol. Sci.* **236**:1–7.
14. Wooley, C.M., et al. 2005. Gait analysis detects early changes in transgenic SOD1(G93A) mice. *Muscle Nerve.* **32**:43–50.
15. Kunst, C.B., Messer, L., Gordon, J., Haines, J., and Patterson, D. 2000. Genetic mapping of a mouse modifier gene that can prevent ALS onset. *Genomics.* **70**:181–189.
16. Graves, J.A. 2006. Sex chromosome specialization and degeneration in mammals. *Cell.* **124**:901–914.
17. Wolach, B., Scharf, Y., Gavrieli, R., de Boer, M., and Roos, D. 2005. Unusual late presentation of X-linked chronic granulomatous disease in an adult female with a somatic mosaic for a novel mutation in CYBB. *Blood.* **105**:61–66.
18. Sakai, T. 1981. The mammalian Harderian gland: morphology, biochemistry, function and phylogeny. *Arch. Histol. Jpn.* **44**:299–333.
19. Chieffi, G., et al. 1996. Cell biology of the harderian gland. *Int. Rev. Cytol.* **168**:1–80.
20. Akiyama, J., et al. 2002. Tissue distribution of surfactant proteins A and D in the mouse. *J. Histochem. Cytochem.* **50**:993–996.
21. Qin, L., et al. 2004. NADPH oxidase mediates lipopolysaccharide-induced neurotoxicity and proinflammatory gene expression in activated microglia. *J. Biol. Chem.* **279**:1415–1421.
22. Gurney, M.E., et al. 1994. Motor neuron degeneration in mice that express a human Cu,Zn superoxide dismutase mutation. *Science.* **264**:1772–1775.
23. Pollock, J.D., et al. 1995. Mouse model of X-linked chronic granulomatous disease, an inherited defect in phagocyte superoxide production. *Nat. Genet.* **9**:202–209.
24. Gavazzi, G., et al. 2006. Decreased blood pressure in NOX1-deficient mice. *FEBS Lett.* **580**:497–504.
25. Alexander, G.M., et al. 2004. Effect of transgene copy number on survival in the G93A SOD1 transgenic mouse model of ALS. *Brain Res. Mol. Brain Res.* **130**:7–15.
26. Gurney, M.E. 1997. The use of transgenic mouse models of amyotrophic lateral sclerosis in preclinical drug studies. *J. Neurol. Sci.* **152**(Suppl. 1):S67–S73.
27. Li, Y., et al. 1998. Validation of lucigenin (bis-N-methylacridinium) as a chemilumigenic probe for detecting superoxide anion radical production by enzymatic and cellular systems. *J. Biol. Chem.* **273**:2015–2023.
28. Li, Q., et al. 2006. Nox2 and Rac1 regulate H2O2-dependent recruitment of TRAF6 to endosomal interleukin-1 receptor complexes. *Mol. Cell. Biol.* **26**:140–154.
29. Harper, S.Q., et al. 2005. RNA interference improves motor and neuropathological abnormalities in a Huntington's disease mouse model. *Proc. Natl. Acad. Sci. U. S. A.* **102**:5820–5825.
30. Volpicelli-Daley, L.A., and Levey, A. 2003. Immunohistochemical localization of proteins in the nervous system. In *Current protocols in neuroscience*. J. Crawley, editor. John Wiley & Sons Inc. Hoboken, New Jersey, USA. 1.2.1–1.2.17.